Journal of Information Systems Engineering and Management
2025, 10(15s)
e-ISSN: 2468-4376
https://www.jisem-journal.com/

Research Article

Little Lime Hydrangea Nanostructure of WO3 films for Gas Sensor and Antibacterial Applications

R. Ravi Kumar, P. Jabbar Khan, D. Sampurna Rao, A. Sivasankar Reddy*

Department of Physics, Vikrama Simhapuri University College, Nellore-524324, Andhra Pradesh, India
**Corresponding Author: akepati77@gmail.com*

ARTICLE INFO

Received: 04 Dec 2024

Revised: 26 Jan 2025

Accepted: 05 Feb 2025

ABSTRACT

In this study, electron beam evaporation was used to prepare nanostructured tungsten trioxide (WO_3) thin films on glass substrates at room temperature and subsequently annealed at different temperatures. The microstructure of the WO_3 films changed from nanoflakes to a little lime hydrangea structure upon variation of the annealing temperature. The surface roughness of the films increased from 14.2 nm (as deposited) to 28.5 nm (673K annealed WO_3). The WO_3 sensor possesses excellent selectivity towards hydrogen gas. The antibacterial activity was experimentally studied using Pseudomonas aeruginosa and this result shows excellent antibacterial activity in annealed WO_3 films.

Keywords: Thin films, Tungsten oxide, Electron beam evaporation, Nanostructure, Gas sensors, Antibacterial.

INTRODUCTION

In the interdisciplinary research area, nanostructured materials play a key role. Researchers are working to prepare the various types of nanostructures to make them more efficient gas sensors and antibacterial activities. The nanostructured metal oxides have been investigated by various research groups using different materials, such as WO_3, SnO_2, TiO_2, ZnO, and Cu_2O, by various synthesis approaches [1] for gas sensors and antibacterial activities. Tungsten oxide (WO_3) has received much attention among these metal oxides, due to its unique properties. WO_3 is a n-type semiconductor with intriguing physical and chemical properties and is potentially useful material in a wide range of applications such as electrochromic, photochromic, photocatalysis, photoluminescence, smart windows, gas sensors, and antibacterial coatings [2-4]. The efficiency of the gas sensor and antibacterial activity of films is attributed to size, thickness, surface area, and stability. WO_3 thin films are prepared using several methods, such as sputtering [5] electron beam evaporation [6], Aerosol assisted chemical vapor deposition [7], and sparking method [8]. To the best of our knowledge, up to now, there is no report on the electron beam evaporated WO_3 thin films for antibacterial (Pseudomonas aeruginosa) applications. In this work, electron beam evaporation was employed to prepare a novel type of nanostructured WO_3 thin films and subsequently annealed at different temperatures, and studied the gas sensor properties and antibacterial activity against Pseudomonas aeruginosa.

MATERIAL AND METHODS

WO_3 pellets are used for the deposition of nanostructured WO_3 thin films on glass substrates via electron beam evaporation. Pellets were synthesized using high-purity WO_3 powder, with a purity level of 99.99%. The distance between the evaporation source and substrate was 7 cm. The parameters maintained during the deposition of the WO_3 thin films are listed in Table 1. The as deposited WO_3 films were post-annealed at 473K, 673K and 723K in air.

Table 1: Parameters maintained during the deposition of the WO_3 films.

Accelerating Voltage	: 48 kV
Accelerating Current	: 1.3 mA

Base Pressure : 3.8 x 10^{-6} mbar

Deposition Pressure : 1 x 10^{-3} mbar

Deposition Time : 10min

Deposition Temperature : Room Temperature

Characterization of WO_3 nanostructured films

Scanning electron microscopy (SEM) was used to examine the microstructure of the films. The surface properties of the films were characterized by atomic force microscopy (AFM). X-ray electron spectroscopy (XPS) is used to study the chemical composition of the films. The thickness of all the as deposited films is around 260nm.

RESULTS AND DISCUSSION

Crystal structure and Microstructure

X-ray diffractometer was used to study the structural properties of the WO_3 films. The as-deposited WO_3 films exhibited an amorphous structure and this structure did not change even after annealing at 673K (Fig.1(a)). From the SEM images, the as deposited WO_3 films exhibited homogenous nanoflakes and were uniformly distributed on the substrate. When the films were annealed at 673K, the microstructure changed, and they showed a little lime hydrangea structure on their surface (Fig. 1(b)). The little lime hydrangea structure is created by stacking the nanoflakes together. The detailed information about the crystal structure and microstructure of the WO_3 films at various annealing temperatures was reported in our previously published paper [6].

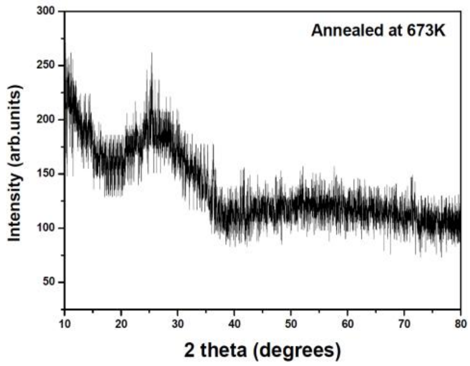

(a)

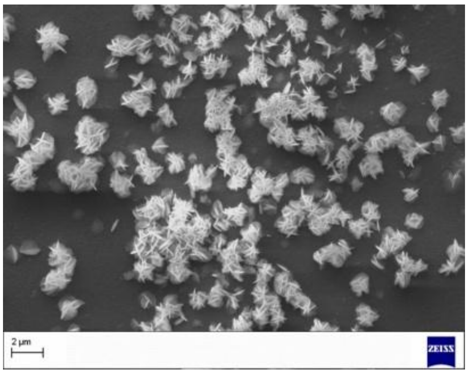

(b)

Figure 1: (a) XRD pattern (b) SEM image of nanostructure WO_3 films annealed at 673K.

Surface morphology

Surface roughness is a key factor influencing optical properties and also gives the quality of the surface, providing some insight into the growth morphology [2]. AFM images of the nanostructured WO_3 films are shown in Fig. 2 (a)&(b). The as deposited films exhibited small sharp peaks and were distributed uniformly (Fig.2(a)). The size of particles increases after annealing the samples as shown in Fig.2(b). The surface roughness of the films increased from 14.2 nm (as deposited) to 28.5 nm (673K annealed WO_3). Ashutosh et al. [9] observed that the grain size and surface roughness of the films increase with annealing temperature, and this is due to the agglomeration of grains taking place at higher temperatures in thermal evaporated WO_3 films.

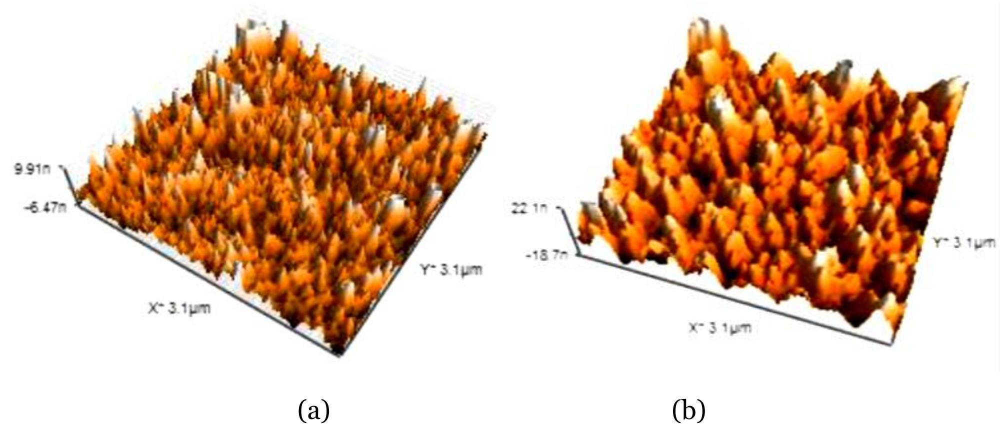

Figure 2: 3D AFM images of nanostructure WO_3 films: (a) as deposited and (b) annealed at 673K.

XPS analysis

The XPS analysis indicates that the only W and O elements are present in WO_3 nanostructure films. Fig. 3 (a) shows the 4f spectrum of the WO_3, revealing chemical states of W with binding energy peaks identified at 35.6 and 37.7 eV, which are associated with W $4f_{7/2}$ and W $4f_{5/2}$, respectively. Fig. 3(b) illustrates the O 1s spectrum, revealing a peak at 529.6 eV. The transition metal oxides exhibit two distinct possibilities for the O 1s peaks: one associated with the O^{2-} peak in the 529.5~530.5 eV range at crystalline sites, and the other peaks attributed to O^- in the 531~532 eV range in the sub-surfaces [10]. After annealing the films at 673K, peaks appeared at 35.1, 37.3 eV, and 529.6 eV related to the W $4f_{7/2}$, W $4f_{5/2}$, and O 1s spectrum, respectively (Figure not shown here). The peaks are slightly shifted towards lower binding energies, indicating the slight changes in the stoichiometry of the WO_3 films. The shift of the Fermi level can be attributed to the increase in oxygen vacancies concentration and the resulting oxygen deficiency in the thin films [11].

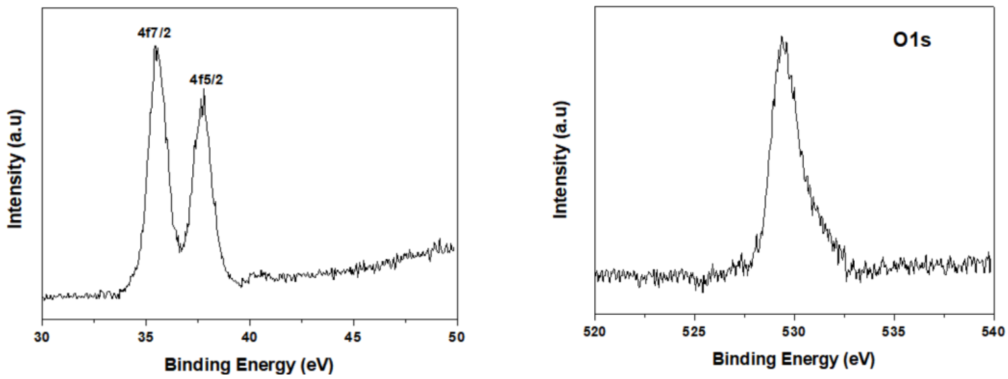

Figure 3: XPS spectra of as deposited nanostructure WO_3 films.

Gas sensor properties

The gas sensing response was measured in a test chamber using a two-probe method to measure the film resistance. The measurement was conducted in a closed chamber with a substrate heater and sample holder. Hydrogen and various alcohol vapors (ammonia, methanol, formaldehyde) were used as target gases to characterize the sensing capabilities of the WO_3 sensors, and the gas flow was regulated and monitored using a mass flow controller. The operating temperature of the sample was managed by a proportional-integral-derivative (PID) controller connected to the heating element on the rear of the sensor holder.

A key factor in assessing a sensor is identifying its optimum operating temperature. In this study, the sensor was tested with the operating temperature range of 30 °C - 300 °C. Fig.4. shows the effect of operating temperature on the hydrogen sensing behavior of WO_3 thin film annealed at 673K. The resistance of gas sensing material decreased significantly with the increase in temperature. The present obtained resistance drop values are 4.23kΩ, 4.75kΩ, and 3.56kΩ, for the operating temperatures of 30^{o}C, 150^{o}C, and 300^{o}C, respectively.

As the operating temperature increases, the target gas molecules exhibit progressively more active, as a result, the resistance drop values are increased. At a higher operating temperature of 300°C, the reduction in resistance is minimal due to the deterioration of the gas diffusion [12].

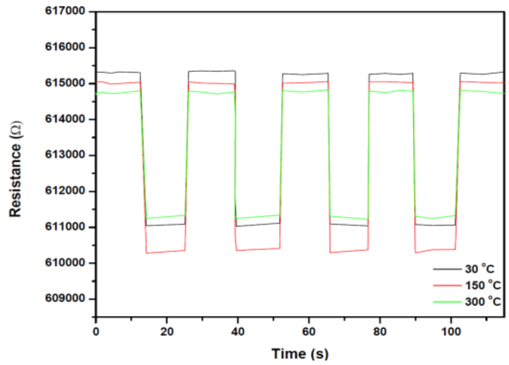

Figure 4: Resistance vs time response of nanostructure WO_3 films annealed at 673K.

Another important parameter of gas sensors is selectivity. In this work, the selectivity of the gas sensor was examined by analyzing the responses to hydrogen, ammonia, methanol, and formaldehyde (Fig.5.). All the gases were evaluated at ambient temperature (30°C) using the same concentration (100ppm). The WO_3 sensor shows outstanding selectivity for hydrogen gas in comparison to the other target gases.

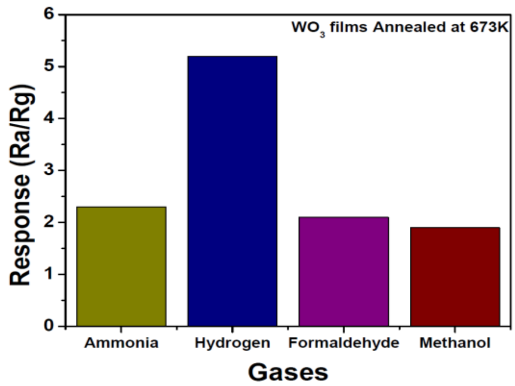

Figure 5: Response of nanostructure WO_3 films of different gases.

Antibacterial properties

Test organism & growth conditions:

Pesudomonas aeruginosa (*P. aeruginosa)* is an opportunistic pathogen that belongs to gram-negative bacteria, which causes a concern for humanity. *P. aeruginosa* (MTCC 424) a gram negative bacteria was obtained from Microbial Type Culture Collection, Chandigarh, India. *P. aeruginosa* is cultured under standard laboratory conditions in LB media at 30°C. The overnight culture was used in this experiment.

The nanostructured WO_3 films antimicrobial activity was assessed using the pore plate technique [13] with slight modification by using LB agar media (Hi-media, India), microorganism being tested were grown on LB broth media. Briefly, the *P. aeruginosa* was cultured on LB broth at 30°C for an overnight period. Subsequently, a loop full of the culture was then inoculated into Mueller Hinton broth (Himedia) and incubated on a rotary shaker at 30°C until the turbidity reached a density equivalent to 0.5 McFarland standard. Following this, 0.25mL of the microorganism was inoculated into molten Muller Hinton agar media and then poured into petri dishes (pour plate method).

Fig.6. shows the antibacterial properties of the as deposited and annealed nanostructured WO_3 films. The antibacterial activity of the nanostructured WO_3 films was evaluated against *P. aeruginosa*. After pouring molten agar MHA media, plates were incubated at 30°C for 24 h. The growth of bacteria around the plate was observed in as deposited film, and it failed to inhibit the growth of *P. aeruginosa* (Fig.6(a)). Whereas, the annealed WO_3 films show antibacterial activity, the bacteria also grow around the plate, except in the WO_3 coating area (Fig.6(b)).

Figure 6: Antibacterial properties of nanostructure WO_3 films: (a) as deposited, (b) annealed at 673K, and (c) uncultured WO_3 films.

CONCLUSIONS

Nanostructured WO_3 films were prepared by the electron beam evaporation technique and studied microstructural, surface morphology, chemical, gas sensor, and antibacterial properties of as deposited and annealed films. The annealing temperature highly influenced the microstructure of the nanostructured WO_3 films. As the annealing temperature was varied, the films microstructure transformed from nanoflakes to a little lime hydrangea structure. The annealing temperature also influenced the surface morphologies of the films. The XPS peaks appeared at 35.6 and 37.7 eV related to W $4f_{7/2}$ and W $4f_{5/2}$, respectively. The gas sensing results indicated that the films annealed at 673K exhibited superior gas sensing characteristics when compared to both the as-deposited films and those annealed at 473K and 723K. The antibacterial efficacy of WO_3 thin films against Pseudomonas aeruginosa was examined. The obtained results indicate that nanostructured WO_3 thin films effectively inhibit the activity of bacteria in the coating area. Electron beam evaporation is a simple and cost-effective method for preparing WO_3 films, which are used in gas sensors and antibacterial coatings.

Acknowledgments

The authors thank Dr. Gopikrishna, Assistant Professor, Department of Zoology, Vikrama Simhapuri University College, Kavali, Andhra Pradesh, India, for providing experimental facilities (Antibacterial studies) in his laboratory.

REFERENCES

[1] Guang-Lei T.; Dan T.; Davoud D.; Azadeh J.; Zhicheng S.; Qian-Qian C. Jos´e Silva P.B.; Xi-Tao Y. Structures, morphological control, and antibacterial performance of tungsten oxide thin films. Ceramics International 2021, 47, 17153 (DOI Link : https://doi.org/10.1016/j.ceramint.2021.03.025)

[2] Ramkumar S.; Rajarajan G. Effect of Fe doping on structural, optical and photocatalytic activity of WO3 nanostructured thin films. J Mater Sci: Mater Electron, 2016, 27, 1847 (DOI Link :https://doi.org/10.1007/s10854-015-3963-6)

[3] Hariharan V.; Radhakrishnan S.; Parthibavarman M.; Dhilipkumar R.; Sekar C. Synthesis of polyethylene glycol (PEG) assisted tungsten oxide (WO3) nanoparticles for l-dopa bio-sensing applications. Talanta 2011, 85, 2166 (DOI Link: https://doi.org/10.1016/j.talanta.2011.07.063)

[4] Duan G.; Chen L.; Jing Z.; De Luna P.; Wen L.; Zhang Zhao L.; et al. Robust Antibacterial Activity of Tungsten Oxide (WO3-x) Nanodots. Chem. Res. Toxicol. 2019, 32, 1357 (DOI Link: doi: 10.1021/acs.chemrestox.8b00399)

[5] Yu L.; Longlong C.; Jiangbin S.; Jinmei B.; Zuming H. Binary solvents of anhydrous ethanol and propylene carbonate for electrolytes of amorphous WO3 films to improve electrochromic performance. Electrochimica Acta 2025, 513, 145542 (DOI Link: https://doi.org/10.1016/j.electacta.2024.145542)

[6] Ravi Kumar R.; Jabbar Khan R.; Sampurna Rao D.; Kalpana G.; Sivasankar Reddy A. Electron Beam Evaporated Nanostructure WO3 Thin Films. Strad Research 2024, 11, 96 (DOI Link: https://doi.org/10.5281/Zenodo.12749339)

[7] Hajimazdarani M.; Javad Eshraghi M.; Ghasali E.; Kolahdouz M. Cost-effective deposition of WO3 films by AACVD method for electrochromic applications: Influence of precursor concentration. Ceramics International 2024, 50, 36872 (DOI Link https://doi.org/10.1016/j.ceramint.2024.07.074)

[8] Thongpan W.; Jumrus N.; Tippo P.; Kumpika T.; Jhuntama N.; Panthawan A.; Rucman S.; Kantarak E.; Sroila W.; Singjai P.; Thongsuwan W. External magnetic field: Enhancing electrochromic efficiency of magnetic metals composited WO3 films prepared by sparking method. Materials Science In Semiconductor Processing 2024, 170, 107970 (DOI Link: https://doi.org/10.1016/j.mssp.2023.107970)

[9] Ashutosh K.; Sunita K.; Debulal K. Influence of annealing temperature on nanostructured thin films of tungsten trioxide. Materials Science in Semiconductor Processing 2024, 17, 43 (DOI Link: http://dx.doi.org/10.1016/j.mssp.2013.07.018)

[10] Jean-Charles D.; Danielle G.; Philippe V.; Alain L. Systematic XPS studies of metal oxides, hydroxides and peroxides. Phys. Chem. Chem. Phys., 2000, 2, 1319 (DOI Link: DOI: 10.1039/a908800h)

[11] Mazur M.; Wojcieszak D.; Wiatrowski A.; Kaczmarek D.; Lubanska A.; Domaradzki J. Piotr M.; Małgorzata K. Analysis of amorphous tungsten oxide thin films deposited by magnetron sputtering for application in transparent electronics. Appl. Surf. Sci. 2021, 570, 151151 (DOI Link: https://doi.org/10.1016/j.apsusc.2021.151151)

[12] Li Z.; Yao ZJ.; Haidry AA.; Plecenik T.; Xie LJ.; Sun LC.; Qawareer F. Resistive-type hydrogen gas sensor based on TiO2: A review Int. J Hydrogen Energy 2018, 43, 21114 (DOI Link: https://doi.org/10.1016/j.ijhydene.2018.09.051)

[13] International Organization for Standardization. 2014. ISO 4833-1:2014. Microbiology of the food chain—horizontal method for the enumeration of microorganisms—part 1: colony count at 30°C by the pour plate technique. International Organization for Standardization, Geneva, Switzerland.